# Simulation and Optimization of Temperature Field for Arc Additive Manufacturing Based on Cloud Computing

Zhibo Yang*

Shenyang Aerospace University, Shenyang, Liaoning, China
*Corresponding author's e-mail: yzbghk@163.com

**Abstract.** With the development of cloud computing technology, it shows unique advantages in high-performance computing applications. In this study, the cloud computing platform AWS was used to simulate and optimize the temperature field during arc additive manufacturing (AM) of 7055 aluminum alloy. The mathematical model of the temperature field is established by defining the thermal physical properties of the material and applying the Fourier heat conduction law and is solved by the finite element method and finite difference method. In the study, the temperature control strategy was optimized by adjusting parameters such as scanning speed, laser power, and cooling system, and the temperature gradient and maximum temperature in the manufacturing process were significantly improved. The results show that the model can effectively predict and control temperature change, and improve the manufacturing precision and material properties. This study demonstrates the application potential of cloud computing in complex industrial simulation and provides the theoretical basis and technical support for efficient arc additive manufacturing.

**Keywords:** Arc additive manufacturing; Temperature field simulation; Cloud computing; 7055 aluminum alloy

## 1 Introduction

Arc additive manufacturing (AM) technology has attracted much attention in the modern manufacturing industry because of its high efficiency and complex structure manufacturing capability. However, precise control of the temperature field is the key to ensuring product quality during the AM process. With the development of cloud computing technology, its powerful data processing capabilities and resource allocation flexibility provide new possibilities for efficient simulation [1]. In this study, the AWS cloud platform was used to simulate and optimize the AM temperature field of 7055 aluminum alloy, and the influence of temperature control on manufacturing accuracy and material properties was explored. Through this research, we aim to demonstrate how cloud computing can help improve the efficiency and product quality of AM technology, and provide a theoretical basis and practical guidance for the advancement of related technologies.

## 2 Model Construction

### 2.1 Cloud Computing Platform Selection and Configuration

Choosing the right cloud computing platform is very important when constructing the temperature field simulation model of arc additive manufacturing. By comparing AWS, Azure, and Google Cloud, the study found that AWS offers a wide range of location-based services and mature security measures, while Google Cloud has advantages in data analytics and machine learning integration, and Azure stands out for its performance in enterprise-class services and hybrid cloud solutions. Based on the consideration of simulation requirements [2], AWS was selected in this study because it has the most balanced performance in terms of processing speed and data security. Specific configuration includes selecting compute instances suitable for HPC, and Amazon EC2 C5 instances, configuring sufficient storage space, utilizing scalable storage provided by Amazon S3, and setting up private virtual networks to ensure the security and stability of data transmission [3]. This configuration ensures an efficient and stable simulation environment so that dynamic changes in the temperature field can be accurately simulated.

### 2.2 Construction of Simulation Model

In constructing the temperature field simulation model of arc additive manufacturing, the physical and thermal-physical properties of 7055 aluminum alloy were first defined, including thermal conductivity of 130 W/m·K, specific heat capacity of 960 J/kg·K, melting point of 635°C, and thermal diffusion coefficient of 25 $mm^2/s$ [4]. Based on Fourier's law of heat conduction, the mathematical model is established by using the heat conduction equation:

$$\frac{\partial T}{\partial t} = \alpha \nabla^2 T + Q \tag{1}$$

where T is the temperature, t is the time, α is the thermal diffusion coefficient, and Q is the heat source intensity per unit volume. The boundary condition settings include a fixed temperature boundary, with the bottom and side boundaries of the model set to 25°C, and an adiabatic boundary at the top of the model where the heat flow derivative is zero. The calculation formula is:

$$T(X,0) = T_0, \frac{\partial T}{\partial n} = 0 \tag{2}$$

where $T_0$ is the initial temperature and $\partial T/\partial n$ is the temperature gradient along the boundary normal. The heat source area simulates arc action, and the heat source intensity is set at 500 $W/cm^3$ [5]. The calculation formula is:

$$Q = Q_0 \cdot exp\left\{-\frac{(X-X_0)^2+(Y-Y_0)^2}{2\sigma^2}\right\} \tag{3}$$

where $Q_0$ is the intensity of the heat source, ($X_0$, $Y_0$) is the central location of the heat source, and σ represents the width of the heat source distribution. For the numerical solution methods, finite element method (FEM) and finite difference method (FDM) were selected, and the Crank-Nicolson method was combined for time integration to ensure the accuracy and efficiency of the simulation. The model is implemented on the AWS cloud platform and uses its high-performance computing resources to carry out spatial grid division and time step setting to accurately simulate the dynamic changes of the temperature field [6]. This comprehensive method takes into account both calculation accuracy and execution efficiency and provides a scientific basis for temperature control in arc additive manufacturing.

## 3 Simulation Process

### 3.1 Experiment Parameters Setup

In the simulation experiment of the temperature field of arc additive manufacturing, the key of the experiment design is to precisely set the parameters to simulate the actual manufacturing environment. In Table 1 below, first, the heating temperature is set to 705°C, slightly higher than the melting point of 7055 aluminum alloy, to ensure that the material can be fully melted. The cooling rate is set at 1 °C/S to simulate the actual cooling environment and help analyze the microstructure and properties of the material after cooling. The layer thickness is set to 0.5 mm, based on the output accuracy of the print head and the level of detail of the required component. In addition, the scanning speed of 10 mm/s is designed to ensure that the material receives sufficient heat while stable deposition, thereby optimizing the mechanical properties and surface quality of the material. Through the precise control of these parameters, the simulation environment can be close to the real manufacturing conditions, to effectively verify and optimize the simulation model of the temperature field on the cloud platform [7].

**Table 1.** Parameter setting.

| Parameter | Set value |
| --- | --- |
| Heating temperature | 705°C |
| Cooling rate | 1 °C/s |
| Layer thickness | 0.5 mm |
| Scanning speed | 10 mm/s |

### 3.2 Experiment Implementation and Data Processing

In the temperature field simulation experiment of arc additive manufacturing, the automatic data collection and processing process on the cloud platform ensures the validity and accuracy of the data. Figure 1 below, by connecting to AWS cloud services, we use APIs to capture key parameters such as temperature data, cooling rate, and layer thickness changes during simulation in real time and automatically store these data in the Amazon RDS database [8]. In the data processing stage, Amazon Athena is used for data query and statistical analysis, including data cleaning, normalization processing, and feature extraction [9]. The processed data was visualized by using the Amazon QuickSight tool, creating dynamic dashboards with temperature profiles and time-temperature curves to visualize the simulation results. In addition, based on the analysis results, the simulation parameters are adjusted through AWS Lambda automation scripts, such as modifying heat source intensity or scanning speed, to optimize the simulation model. This automatic data collection and processing process not only improves the experimental efficiency but also enhances the science and practicability of simulation [10].

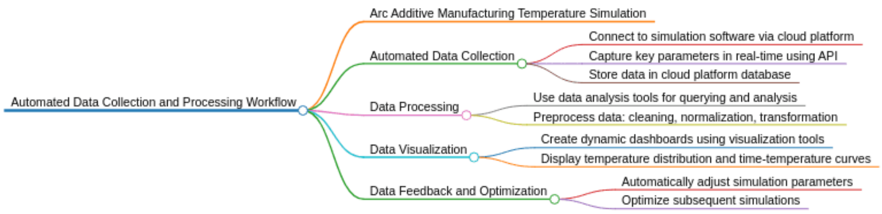


**Fig. 1.** Data collection and processing workflow.

# 4 Experimental Results

## 4.1 Display of Simulation Results

In the temperature field simulation experiment of arc additive manufacturing, we analyzed the temperature distribution and variation in detail through the data collected at nine monitoring locations. In Figure 2, at the beginning of the simulation, the temperature at all locations was room temperature 25°C, showing the consistency of the initial state. As the time progresses to 60 seconds, the temperature at Positions 2 and 5 rises to 300°C, and these regions are the hottest due to the high heat source. At 120 seconds, the temperature at Position 5 rises to 450°C, making it the hottest zone. By 180 seconds, the peak temperature at Position 5 reached 700°C, indicating a high-temperature state under continuous heating. During the 240 and 300-second cooling phases, the temperature at each position was gradually reduced, from 700°C to 400°C at Position 5, demonstrating an effective cooling process. Through these time-temperature curves (Figure 3), we observe how the temperature at each monitoring point changes over time, with Location 5 showing the fastest rate of temperature rise and a slower rate of cooling, possibly due to heat source proximity or heat accumulation effects.

In the analysis of the simulation results of the temperature field of arc additive manufacturing, the effects of temperature extremes and distributions, cooling rates, and temperature gradients are investigated in detail. Temperature extremes, especially the high temperature of 700°C observed at Position 5, lead to a significant expansion of the heat-affected region of the material, which significantly changes the microstructure of the material, for example through grain coarsening, which in turn affects the mechanical properties of the material. In terms of cooling rate, the central region cools faster than the edge region, and this rapid cooling leads to uneven solidification of the material, increasing the residual stress and affecting the overall mechanical properties of the material. In addition, through the plotted temperature distribution map, we see the temperature differences between different regions in the simulation process, and the regions with high-temperature gradients are prone to thermal stress and local deformation during the material deposition process. The fine-tuning and optimization of these temperature controls are key to improving the quality and reliability of the manufactured parts.

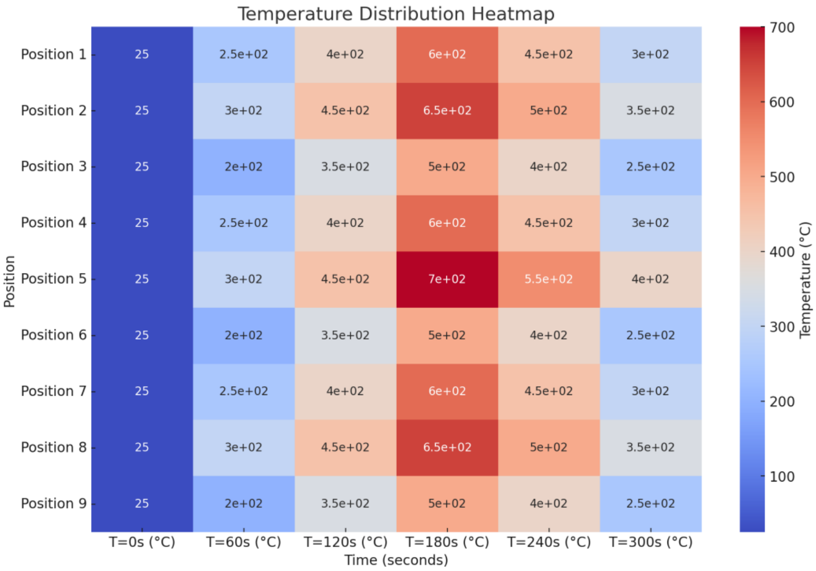


**Fig. 2.** Temperature distribution heat map.

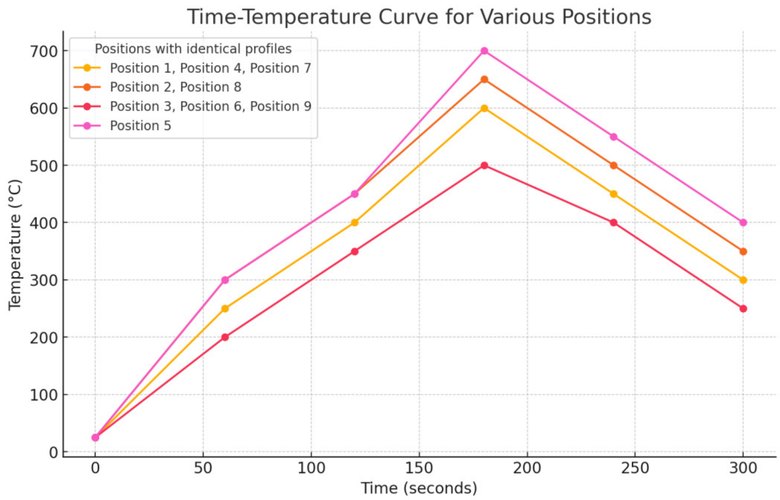


**Fig. 3.** Time-temperature curve.

### 4.2 Display of Simulation Results

Aiming at the problem of temperature control in the arc additive manufacturing process, we have developed a series of specific optimization strategies according to the detailed simulation results. We adjust the scanning speed and power, increase the scanning speed from the original 10 mm/s to 15 mm/s, and reduce the laser power from the original 200 W to 180 W. This adjustment is designed to reduce the heat input per unit area, control the maximum temperature in the high-temperature area, and avoid overheating of the material. Improved cooling system design: Additional cooling channels were installed in key high-temperature areas and a more efficient cooling medium (from water-based coolant to argon) was adopted. These improvements can improve the cooling efficiency of these areas, accelerating the cooling rate to 1.5 °C/s. Interlayer wait time optimization: Increasing the wait time from 30 to 45 seconds after each layer is printed allows the material more time to cool before each layer is applied, reducing the temperature gradient between the layers and thus reducing heat accumulation (Table 2).

**Table 2.** Model optimization comparison.

| Parameter/Result | Before optimization | After optimization | Change |
|---|---|---|---|
| Maximum temperature (°C) | 700 | 650 | -50°C |
| Cooling rate (°C/s) | 1.00 (central area) | 1.25 (central area) | +0.25 °C/s |
| Temperature gradient (°C/mm) | 50 | 30 | -<br>20 °C/mm |
| Inter-layer temperature difference (°C) | 40 | 20 | -20°C |

## 5 Conclusion

In this study, cloud computing technology is successfully applied to simulate and optimize the temperature field in arc additive manufacturing. Through detailed model building and simulation processes, we not only improve the accuracy of temperature control but also significantly improve thermal management in the manufacturing process through optimization strategies. The techniques used in the study include adjusting the scanning speed and power, improving the cooling system, and optimizing the interlayer wait time, all of which effectively reduce the maximum temperature and temperature gradient and reduce the thermal stress of the material. The results show that these optimization measures have a significant impact on improving the quality and performance of the final product. Therefore, cloud computing shows great potential in improving the efficiency and product quality of arc additive manufacturing, providing a valuable reference and practical basis for the development of related technologies in the future.

## References


1. WANG L., ZHANG Z., XU D., et al. Numerical simulation and mechanism study of grain refinement during double pulsed wire arc additive manufacturing [J]. Transactions of the China Welding Institution, 2019, 40 (4): 137-140.
2. WANG H., HUANG J., CHEN S., et al. Analysis of the theory and temperature field of additive manufacturing with powder core wire based on Cu-Al-Fe alloy [J]. Transactions of the China Welding Institution, 2023, 44 (4): 111-119.
3. WU X., LUO W., WANG Y., et al. Simulation on friction stir welding 7055 aluminum alloy based on CEL model [J]. Transactions of the China Welding Institution, 2021, 42 (7): 44-50, 59.
4. WU X., LIN H., WANG Y., et al. The microstructure evolution in the nugget zone of Q&P980 steel joints under the condition of friction stir welding thermal-mechanical couple effects [J]. Transactions of the China Welding Institution, 2023, 44 (6): 120-128.
5. WANG J. S. and JI L. S. Effect of scanning speed on temperature field of laser cutting 6061 aluminum alloy sheet [J]. Manufacturing Technology & Machine Tool (6): 39-43.
6. GAO Q., LI W. B., and GUO G. Y. Simulation and Experimental Study on Temperature Field in Micro-milling of Single Crystal Nickel-based Superalloy [J]. Machine Tool & Hydraulics, 2022, 50 (2): 65-69.
7. Wang L., Xie L. Y., Zhang D., et al. Dynamic simulation of temperature field during friction stir welding [J]. Journal of Northeastern University (Natural Science), 2008, 29 (7): 1, 025.
8. Zhu J., Wang H., Shi D., et al. Element loss behavior and compensation of additive manufacturing memory alloy [J]. TRANSACTIONS OF THE CHINA WELDING INSTITUTION, 2022, 43 (9): 50-55.
9. LIANG H., LI P., SHEN X., et al. Finite element analysis of the effect of ultrasonic impact on the stress of aluminum alloy arc additive manufacturing [J]. Transactions of the China Welding Institution, 2023, 44 (10): 79-85, 119.
10. WANG F., SONG Y., and ZHANG J. Detailed effect of the spot-welding process on spot quality of high-strength aluminum alloy used in astronavigation [J]. TRANSACTIONS OF THE CHINA WELDING INSTITUTION, 2010 (12): 37-40, 44. Multivariate Data Analysis in Ecology and Systematics. SPB Publishing, The Hague.